Generation of OAM Beam with High Azimuthal Symmentry through Planar UCA for Vehicular Communication

Y. Mallikharjuna Reddy, U. V. Ratna Kumari
Department of Electronics and Communication Engineering, jawaharlal nehru technological university kakinada, Andhra Pradesh, India.
Y. Mallikharjuna Reddy (e-mail: ymreddy2@gmail.com)

ABSTRACT In this paper, a uniform circular array (UCA) with circularly polarized (CP) square patches is presented for the generation of orbital angular momentum (OAM) beam with high azimuthal symmetry. The proposed CP UCA is a compact structure with a simple feed network generating OAM beams. The design consists of eight circularly polarized square patch antennas which are geometrically rotated to obtain the required phase distribution. The left hand circularly polarized square patch used as a radiating element in UCA exhibits l = + 1 OAM mode, while the right hand circularly polarized square patch exhibits l = - 1 OAM mode. In addition, the antenna exhibits a single-layer structure, which facilitated the fabrication of the design and reduced the cost as well. The simulated and measured results are reported showing that the antenna exhibits an OAM beam of l = + 1 and l = - 1 modes at 5.85 GHz with high azimuthal symmetry. The mode purity estimation is also reported for the OAM l = + 1 and l = - 1 modes. The gain of the conical shaped OAM beam is almost 11 dBi which makes it quite viable for applications in wireless and vehicular communications.

INDEX TERMS Azimuthal symmentry, Circular polarization (CP), Orbital angular momentum (OAM), Unifrom circular array (UCA).

I. INTRODUCTION

Emerging wireless communication systems have resulted in a substantial growth in the demand for increased data rates over the past few years [1]. This has contributed to the development of various multiplexing techniques depending on the diversity of polarization, frequency, and space, all of which can enhance spectral efficiency [2]. In contrast to these prior techniques, a distinct approach that relies on the utilization of microwaves bearing orbital angular momentum (OAM) has been proposed [3]. OAM beams with vortex wavefronts have received much interest from the initial studies in the optical domain and later the subsequent utilization at radio frequencies [4]. These beams have the potential to theoretically contain an infinite number of mutually orthogonal eigenstates along with helical phase fronts of $\exp(jl\phi)$, where ϕ is azimuthal angle and l is the integral topological charge. These eigenstates are characterized as OAM modes based on different values of topological charge ($\mathrm{l}= 0, \pm1, \pm2, ..$). The multiplexing of various OAM modes enables the transmission of multiple channels of signals on a single frequency [5]. Therefore, OAM-based communications have the capability to enhance channel capacity and spectral efficiency. In addition, the conical shaped pattern of the OAM beam along with high azimuthal symmetry provides a wide range of coverage area for communication with multiple signals simultaneously. OAM waves naturally have a cone-shaped pattern of radiation, and M. Veysi *et al.* showed that a cone-shaped OAM wave could also be employed in future vehicular communications [6].

Initially, OAM beam generation was demonstrated using spiral phase plates [7], and then with reflector antennas [8]. But due to complications in practical realization, these methods were regarded as not compatible for OAM beam generation. Consequently, microstrip patch antennas with slots were demonstrated for the generation of OAM beams, however there is a limitation of multiple layers and multiple feeds [9]. Concurrently, a simple approach for generating OAM beams employing uniform circular arrays(UCA) was proposed. UCA consists of circularly arranged patch antennas with each radiating element corresponding to different phase [10]. This technique became reliable due to its simple practical realization and low-cost effectiveness. The use of linearly and circularly polarized (CP) patch antennas as radiating elements offers two distinct UCA approaches. Although, circular array of linearly polarized patch antennas is a general approach of UCA for generating OAM beams, it has a limitation of requiring increased feed length for required phase distribution. In the second approach, the required phase variation in UCA is investigated through the geometrical rotation of CP patch antennas. So far, different approaches were proposed for the generation of OAM beam using UCA

with CP patches. Initial approach of CP UCA was introduced for generating dual mode OAM beams [11]. Later, reconfigurable CP UCA's were introduced for generating multiple modes of OAM beams [12], [13]. These investigations have the limitation of multiple layered structure and low azimuthal symmetry.

In this paper, a single-layer UCA with CP square patches for generating OAM beam of modes l = + 1 and l = - 1 at 5.85 GHz with high azimuthal symmetry is presented. The design of the CP square patch antenna and the UCA with CP square patches for OAM generation were discussed in section II. The section III gives details of simulated and measured results of the UCA for OAM modes l = + 1 and l = - 1 along with the mode purity estimation. Lastly, conclusions were discussed in section IV.

II. ANTENNA

A. CP SQUARE PATCH ANTENNA

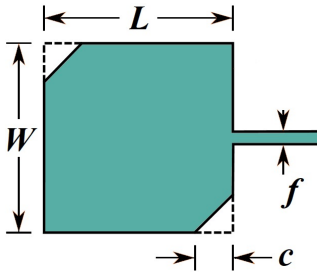

FIGURE 1: The geometry of CP cut corner square patch

Microstrip patch antennas can be made to exhibit CP by either altering the radiating patch's geometry or subjecting the radiating element to multiple feeds. For the proposed square patch, CP is achieved by cutting the ends of opposite corners to attain quadrature phase coupling between both the orthogonal TM_{01} and TM_{10} modes [14] [15]. The direction of cut corner is crucial in conversion between the two states of CP. To exhibit left hand circular polarization (LHCP), the corner adjacent to $(+ve)x$ direction of feed point is cut along with its diagnol corner. In the same way, when the corner of patch adjacent to $(-ve)x$ direction of feed point along with its diagnol corner is cut, the square patch exhibits right hand circular polarization (RHCP).

The proposed square patch antenna with cut corners is shown in Figure 1. The square patch is designed with the dielectric material FR-4 as substrate with a dielectric constant of 4.3, thickness of 1.6 mm along with an input impedance of 100 Ω. The dimensions of radiating element are W = 12.21 mm, L = 12.21 mm, c = 1.41 mm and f = 0.83 mm. From the Figure 2, it can be observed that the simulated reflection coefficients of the LHCP and RHCP cut corner square patches resonate at 5.6 GHz. In the Figure 2 the axial ratio of LHCP and RHCP cut corner square patches at the resonant frequency is less than 3 dB, which confirms that it exhibits CP. The surface current distributions of the proposed

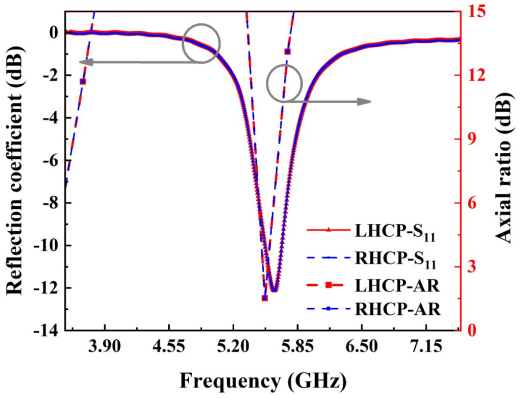

FIGURE 2: Simulated reflection coefficient and Axial ratio of LHCP and RHCP square patches

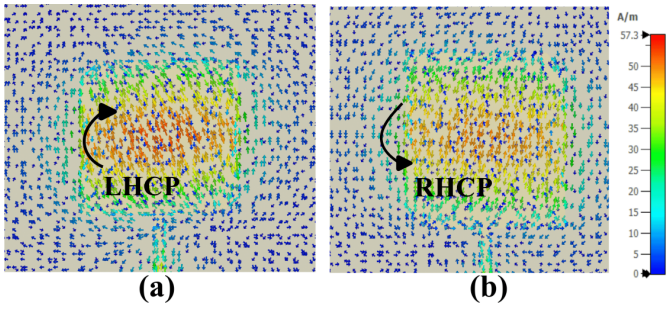

FIGURE 3: Surface current distribution of square patches at 5.6 GHz (a) LHCP and (b) RHCP.

square patches at 5.6 GHz are shown in Figure 3. The clockwise rotation of the field in the square patch radiates LHCP (Figure 3a), whereas the anticlockwise rotation radiates RHCP (Figure 3b). The simulated normalized farfield cuts of both LHCP and RHCP square patches at resonant frequency of 5.6 GHz are depicted in the Figure 4.

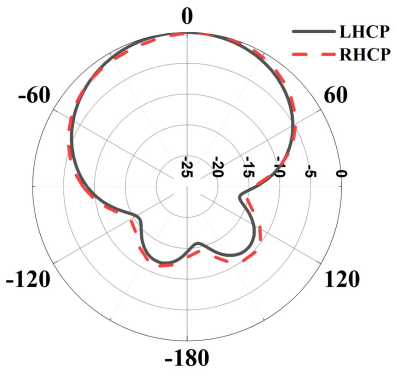

FIGURE 4: The normalized radiation pattern of both LHCP and RHCP square patches at 5.6 GHz

B. UCA DESIGN

The proposed structure of UCA is implemented with each element in the array having an incremental phase of $\Delta\phi = 2\pi l/N$ degrees where, N is the number of radiating elements [16]. This phase shift among all the radiating elements in the array constitutes the OAM beam generation with a 0^o to 360^o phase distribution around the UCA. To accomplish this, the array's feed network must be designed such that each element has a longer feed length than the others. Adjusting the lengths of the feed lines is a complicated process because it must be done within the smaller circular array of radius, the optimized array radius $r = 0.5\lambda$ chosen based on the number of array elements and to reduce the divergence angle of the OAM wave. Thus to avoid this complicated design procedure, a modified structure of UCA which does not involve feed length increment for phase variation to generate OAM beams is necessary. The utilization of CP antennas as a radiating element in the UCA provided a better solution for simplifying the feed network [17]. This is due to the fact that OAM beams can be generated by a circular array of CP patch antennas with a phase delay of $l.\Delta\varphi$ between the feed points of each radiating patch, where l is the order of OAM mode, $\Delta\varphi = 2\pi/N$ and N is the number of elements.

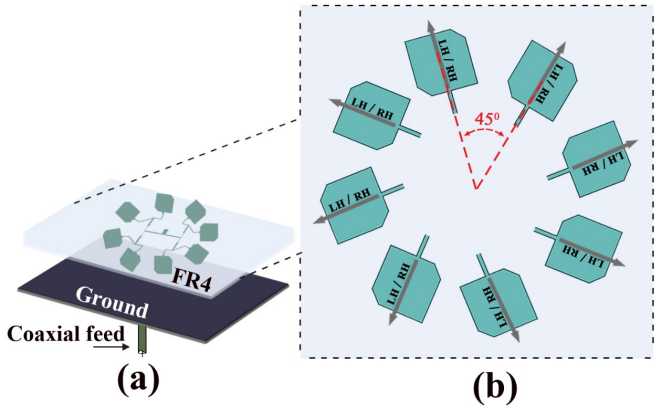

FIGURE 5: The structure of UCA with CP cut corner square patches

In the desired array configuration, the square patch antennas are aligned with their feed points towards the array's center. This enables for the phase delay of $l.\Delta\varphi$ to be maintained between any pair of elements. According to the relation $-N/2 < l < N/2$, number of elements in UCA is dependent on OAM mode 'l' . Consequently, eight radiating elements were chosen to be optimal number in UCA for generating OAM modes of l = + 1 and l = - 1 with high mode purity. The Figure 5. depicts the arrangement of desired UCA design with CP corner cut square patches. To generate the l=+1 OAM mode, eight LHCP cut-corner square patches were positioned in the UCA so that the feeds of adjacent elements were out of phase by a factor of $l.\Delta\varphi$ = + 45^o. The required phase at each radiating element for l = + 1 OAM beam is

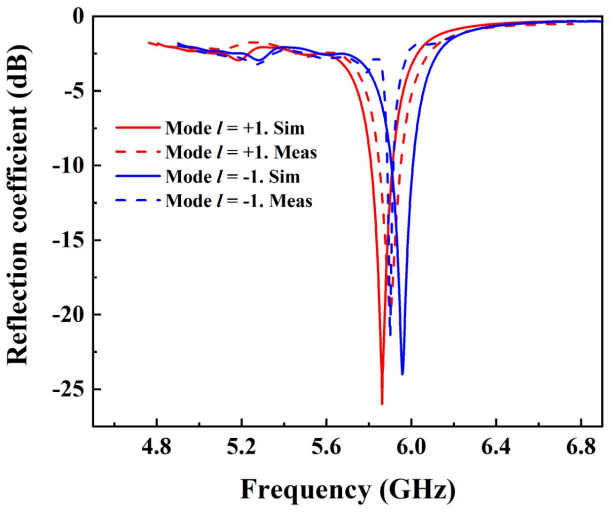

FIGURE 6: The simulated and measured reflection coefficients of CP UCA with square patches

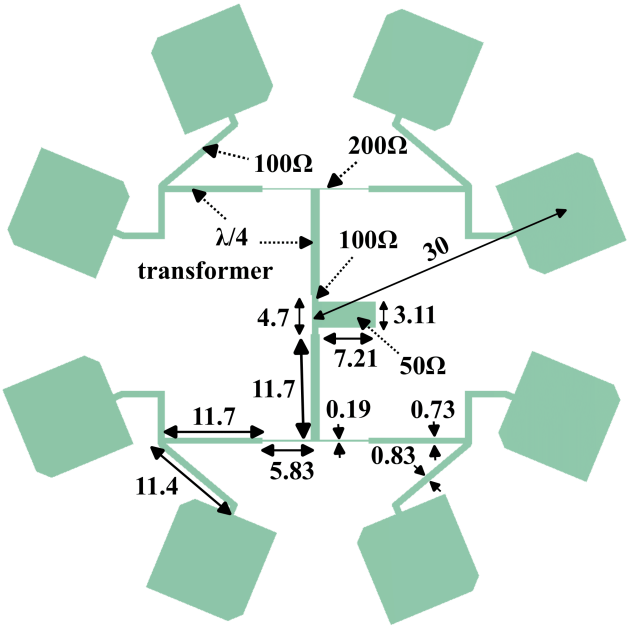

FIGURE 7: The configuration of the eight-element UCA feed network(all dimensions are in mm).

obtained by the clockwise rotation of the CP square patch antenna. Accordingly, the phase shift exerted by radiating elements allows for the generation of a conventional OAM beam of mode l = + 1 when the UCA is excited via a coaxial feed. With a phase difference of $l.\Delta\varphi$ = - 45^o between the feed locations of each element, the LHCP square patch in UCA is replaced out for RHCP square patches to generate OAM mode l= - 1. Figure 7. displays the eight-element UCA's designed feed network. The proposed design has a 30 mm radius for the UCA.

III. RESULTS AND DISCUSSION

An illustration of the simulated and measured reflection coefficients of the proposed UCA is shown in the Figure 6. For both modes, the mutual coupling effect of radiating elements in the UCA causes the center frequency to be shifted from 5.6 GHz to 5.85 GHz. The S_{11} for both l = + 1 and l = - 1 modes are less than -15 dB at 5.85 GHz. Due to helical phase fronts present in OAM beams, they have a distinct phase singularity at their centers. This effect causes the radiation pattern of an OAM beam to look like a doughnut with a null in the middle when viewed from z-axis in boresight direction. The Farfield 3D radiation patterns in Figure 8 show that they have a null in the center confirming that the generated beams have OAM property. In addition,

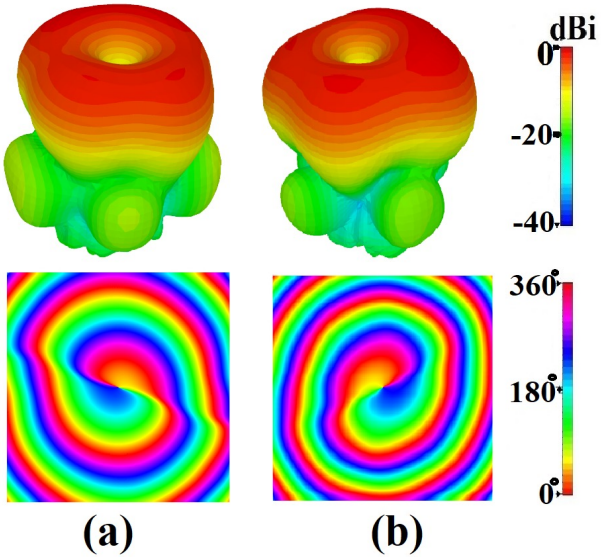

FIGURE 8: The simulated magnitude of the radiation pattern along with E-field phase distribution in z-plane for l = + 1 and l = - 1 modes

the plots show that amplitudes of radiation pattern at either side of center are exactly on same level owing to the high azimuthal symmetry with divergence angle of $\pm 24^{o}$. It can be observed in the Figure 8(a), the phase distribution of E-field in the z-plane is oriented in clockwise direction, confirming the l = + 1 OAM mode generation. The vice versa of the latter in Figure 8(b), confirms the generation of l = - 1 OAM mode. The OAM spectrum is determined by taking samples of the OAM beam in the z-plane and applying a discrete Fourier transform. The following expressions describes the Fourier relationship between the OAM spectrum P(α) and the corresponding sample phase $\psi(\varphi)$ [18].

$$P(\alpha) = \frac{1}{2\pi}\int_{0}^{2\pi} \psi(\varphi) d\varphi exp(-jl\varphi) \tag{1}$$

$$\psi(\varphi) = \sum_{-\infty}^{\infty} P(\alpha) exp(jl\varphi) \tag{2}$$

here, $exp(jl\varphi)$ represents the harmonics correlated with the UCA, whereas $\psi(\varphi)$ represents the fractional sampling phase value in the sampling plane. The z-plane electric field responses are normalized to energy weights.

$$\text{energy weight of OAM mode } (l) = \frac{A_l}{max\left[A_{l'}\right]_{\ l'=-4\ to\ 4}} \tag{3}$$

Fourier transform is applied to these normalized weights to estimate the mode purity of the OAM modes l = + 1 and l = - 1. The above sequence of steps is used in developing a python script such that the E-field phase values of particular OAM mode in z-plane were given as inputs. The resulting plots provides the maximum amplitude at corresponding OAM mode order. The mode purity of the simulated radiation patterns is plotted as shown in the Figure 9, where it is evident that the amplitude of spectra at the corresponding modes of l = + 1 and l = - 1 is maximum.

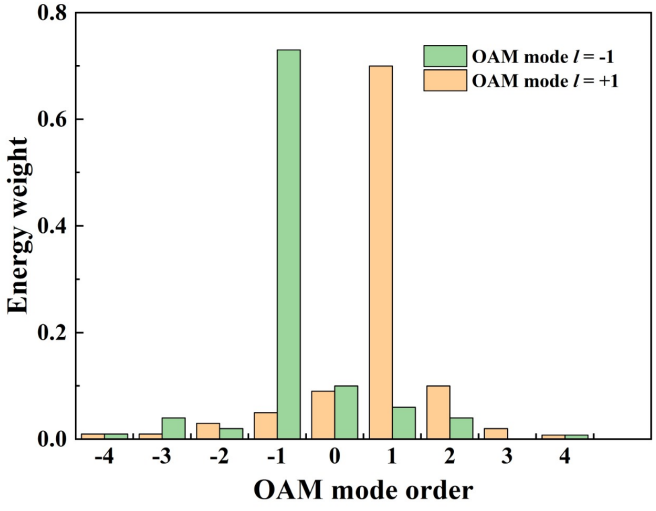

FIGURE 9: Simulated mode purity of OAM beams of l = + 1 and l = - 1 modes

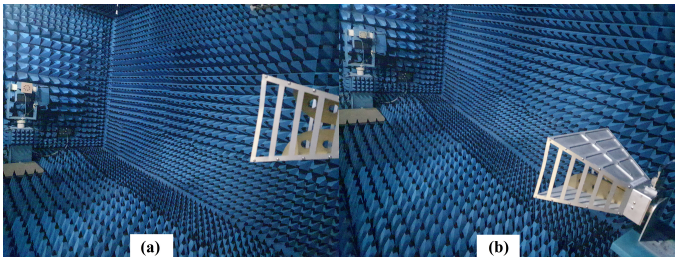

FIGURE 10: Experimental setup for measuring OAM beam (a) l = +1 OAM mode, and (b) l = -1 OAM mode.

A. FABRICATION AND EXPERIMENTAL RESULTS

For experimental verification of the proposed design, a printed circuit board model of the UCA is fabricated and

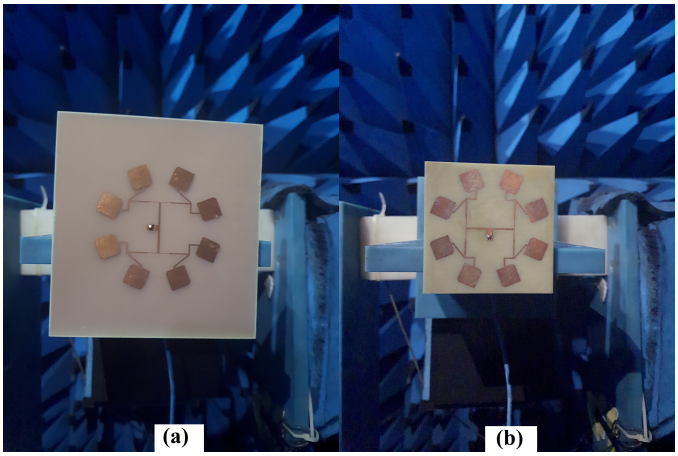

FIGURE 11: Fabricated prototype of the UCA (a) l = +1, and (b) l = -1.

measured in an anechoic chamber as shown in the Figures 10 and 11. The measurement receiver is a horn antenna with ultra-wideband capability. The simulated and measured 2D radiation patterns of both l = + 1 and l = - 1 OAM modes at 5.85 GHz in elevation and azimuthal plane are depicted in the Figure 12. The 3-dB beamwidth in elevation plane is observed to be 20^o to 28^o and 19^o to 27.2^o for both the modes. In elevation and azimuthal planes, co-polarized field is observed to be 20 dB stronger than cross-polarized field. The plots in the Figure 13 depicts the measured and simulated

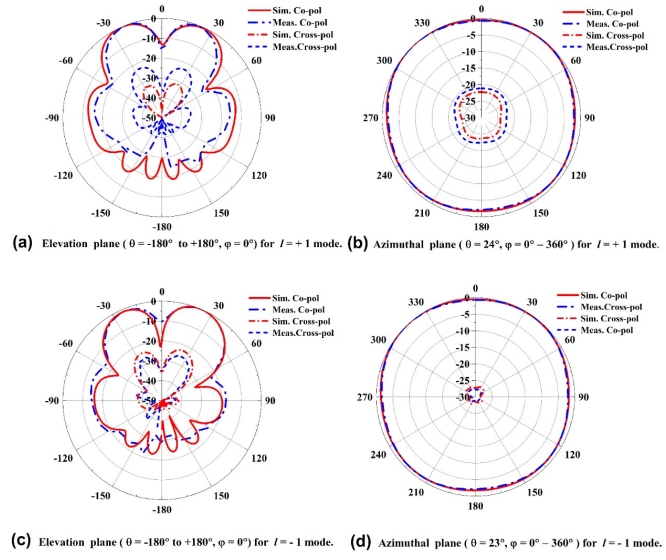

FIGURE 12: Simulated and measured normalized radiation patterns at 5.85 GHz.

gain at resonant frequency for both l = + 1 and l = - 1 OAM mode structures. For the l = + 1 mode, the simulated peak gain is 11.8 dBi and the measured peak gain is 10.2 dBi, respectively. For the l = - 1 mode, the simulated peak gain is 10.4 dBi and the measured peak gain is 10 dBi, respectively.

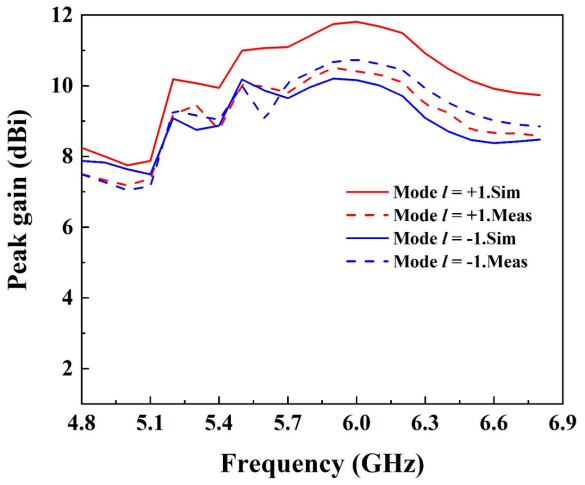

FIGURE 13: The simulated and measured gain plots of l = +1 and l = - 1 OAM modes.

OAM modes l = +1 and l = -1 have the same fabricated model dimensions except for substrate area, which may cause a slight difference in farfield radiation patterns. Complications with the experimental setup are liable for any differences that may be observed between simulated and measured results.

IV. CONCLUSION

A circularly polarized UCA for the generation of OAM modes l = + 1 and l = - 1 without the use of a phase increment approach in feed network on a single layer. The design consists of eight cut corner square patch antenna as radiating elements for generating OAM beam at 5.85 GHz. The far-field radiation patterns of the proposed designs have null in the center, confirming the OAM beam property and exerting high azimuthal symmetry.. The peak gain for both OAM l = + 1 and l = - 1 mode designs is reported to be in the range of 10 dBi - 11.8 dBi. The mode purity estimation is also reported which ensures better OAM mode generation by the proposed UCA designs. Hence, the potential of proposed UCA for generating OAM beam with azimuthal symmetry can be used in variety of applications pertaining to vehicular communications.

REFERENCES

[1] J. R. Bhat and S. A. Alqahtani, "6g ecosystem: Current status and future perspective," IEEE Access, vol. 9, pp. 43 134–43 167, 2021.

[2] J. Reed, M. Vassiliou, and S. Shah, "The role of new technologies in solving the spectrum shortage [point of view]," Proceedings of the IEEE, vol. 104, no. 6, pp. 1163–1168, 2016.

[3] S. M. Mohammadi, L. K. Daldorff, J. E. Bergman, R. L. Karlsson, B. Thidé, K. Forozesh, T. D. Carozzi, and B. Isham, "Orbital angular momentum in radio—a system study," IEEE transactions on Antennas and Propagation, vol. 58, no. 2, pp. 565–572, 2009.

[4] L. Allen, M. W. Beijersbergen, R. Spreeuw, and J. Woerdman, "Orbital angular momentum of light and the transformation of laguerre-gaussian laser modes," Physical review A, vol. 45, no. 11, p. 8185, 1992.

[5] J. Wang, J.-Y. Yang, I. M. Fazal, N. Ahmed, Y. Yan, H. Huang, Y. Ren, Y. Yue, S. Dolinar, M. Tur et al., "Terabit free-space data transmission

employing orbital angular momentum multiplexing," Nature photonics, vol. 6, no. 7, pp. 488–496, 2012.
[6] M. Veysi, C. Guclu, F. Capolino, and Y. Rahmat-Samii, "Revisiting orbital angular momentum beams: Fundamentals, reflectarray generation, and novel antenna applications," IEEE Antennas and Propagation Magazine, vol. 60, no. 2, pp. 68–81, 2018.
[7] P. Schemmel, G. Pisano, and B. Maffei, "Modular spiral phase plate design for orbital angular momentum generation at millimetre wavelengths," Optics express, vol. 22, no. 12, pp. 14 712–14 726, 2014.
[8] W. J. Byun and Y. H. Cho, "Generation of an orbital angular momentum mode based on a cassegrain reflectarray antenna," in 2017 IEEE International Symposium on Antennas and Propagation USNC/URSI National Radio Science Meeting, 2017, pp. 1191–1192.
[9] M. Barbuto, F. Trotta, F. Bilotti, and A. Toscano, "Circular polarized patch antenna generating orbital angular momentum," Progress In Electromagnetics Research, vol. 148, pp. 23–30, 2014.
[10] Z.-G. Guo and G.-M. Yang, "Radial uniform circular antenna array for dual-mode oam communication," IEEE Antennas and Wireless Propagation Letters, vol. 16, pp. 404–407, 2017.
[11] X.-D. Bai, X.-L. Liang, Y.-T. Sun, P.-C. Hu, Y. Yao, K. Wang, J.-P. Geng, and R.-H. Jin, "Experimental array for generating dual circularly-polarized dual-mode oam radio beams," Scientific reports, vol. 7, no. 1, pp. 1–8, 2017.
[12] Z.-G. Guo, G.-M. Yang, and Y.-Q. Jin, "Circularly polarised oam antenna using an aperture-coupled uniform circular array," IET Microwaves, Antennas & Propagation, vol. 12, no. 9, pp. 1594–1600, 2018.
[13] L. Li and X. Zhou, "Mechanically reconfigurable single-arm spiral antenna array for generation of broadband circularly polarized orbital angular momentum vortex waves," Scientific reports, vol. 8, no. 1, pp. 1–9, 2018.
[14] S. Baudha and V. Dinesh Kumar, "Corner truncated broadband patch antenna with circular slots," Microwave and optical technology letters, vol. 57, no. 4, pp. 845–849, 2015.
[15] Y. Huang, L. Yang, J. Li, Y. Wang, and G. Wen, "Polarization conversion of metasurface for the application of wide band low-profile circular polarization slot antenna," Applied physics letters, vol. 109, no. 5, p. 054101, 2016.
[16] Q. Bai, A. Tennant, and B. Allen, "Experimental circular phased array for generating oam radio beams," Electronics letters, vol. 50, no. 20, pp. 1414–1415, 2014.
[17] K. Bi, J. Xu, D. Yang, Y. Hao, X. Gao, and S. Huang, "Generation of orbital angular momentum beam with circular polarization ceramic antenna array," IEEE Photonics Journal, vol. 11, no. 2, pp. 1–8, 2019.
[18] B. Jack, M. J. Padgett, and S. Franke-Arnold, "Angular diffraction," New Journal of Physics, vol. 10, no. 10, p. 103013, oct 2008.